Zucca, M., & Valente, M. (2020). On the limitations of decoupled approach for the seismic behaviour evaluation of shallow multi-propped underground structures embedded in granular soils. *Engineering Structures*, 211, 2020. ISSN 0141-0296.

https://dx.doi.org/10.1016/j.engstruct.2020.110497

ON THE LIMITATIONS OF DECOUPLED APPROACH FOR THE SEISMIC BEHAVIOUR EVALUATION OF SHALLOW MULTI-PROPPED UNDERGROUND STRUCTURES EMBEDDED IN GRANULAR SOILS

Marco ZUCCA[1*], Marco VALENTE[2]

[1]Department of Architecture, Built Environment and Construction Engineering
Politecnico di Milano
e-mail: marco.zucca@polimi.it

[2]Department of Architecture, Built Environment and Construction Engineering
Politecnico di Milano
e-mail: marco.valente@polimi.it

ABSTRACT

The evaluation of the seismic behaviour of shallow multi-propped underground structures (e.g. metro stations, parking, etc.) can be considered as one of the most important and actual research topics in structural earthquake engineering. Over the last decades, different types of analysis approaches have been proposed, but several issues are still open, especially for multi-propped structures embedded in granular soils. In this paper, the main limitations of the decoupled approach are investigated and discussed through a large set of numerical simulations involving: i) a multi-propped underground structure; ii) five natural and one synthetic accelerograms; iii) four different soil profiles characterized by the same mechanical properties but different values of the shear modulus that are related to the shear wave velocity ranging between 360 m/s and 750 m/s. The results, in terms of bending moment acting on RC retaining walls, obtained through the decupled approach are discussed in comparison with those obtained through the coupled approach (non-linear dynamic analysis), highlighting the main differences and limitations. This study shows that the decoupled approach provides consistent results only for soil profiles characterized by low values of stiffness due to the main assumptions underlying the approach.

KEYWORDS: *underground structures; decoupled approach; seismic response; time history analysis.*

1. INTRODUCTION

Over the last decades, different types of underground structures classifications have been provided considering the construction method [1] and the intended use [2], but despite such differences in terms of construction methods and structural characteristics, the seismic response of such structures is generally dominated by similar parameters.

The damaging effects of strong earthquakes on underground structures can be classified into two main groups: damages caused by soil shaking and damages due to soil failures [30]. As a result of the seismic waves propagation generated by an earthquake, the soil will undergo vibrations that are manifested as soil shaking [31]: consequently, underground structures will suffer more or less deformations simultaneously with the soil deformations. The second major group includes a broad spectrum of different failure modes, such as faulting and tectonic uplift, liquefaction, subsidence and slope instabilities.

For a long period, however, underground structures have been considered practically invulnerable to seismic actions. Such a belief about their safety has been undermined by the serious and extensive damages suffered by such structures, in the case of not adequate seismic design, during recent strong earthquake events [3], including the 1995 Kobe (Japan), the 1999 Chi-Chi (Taiwan), the 1999 Kocaeli (Turkey) and the 1999 Athens (Greece) earthquakes [4]. In particular, the collapse of the Daikai metro station, which occurred during the above-mentioned Kobe earthquake, was emblematic: the central columns collapsed because they were designed to resist only vertical loads, Fig. 1, [5].

For these reasons, several Technical Codes have recently started paying particular attention to the seismic design of such structures [26,27], and in the same way, in the last few years, several researchers have developed different methods to evaluate the seismic behaviour of underground structures in the transversal [7-19] and longitudinal [2,11,20,21,22,23] directions, including coupled and decoupled approaches: in addition, some comparisons between the different methods have been carried out [24,25]. An important research has been conducted in [28] to obtain fragility curves for the seismic characterization of underground structures. Despite such developments, various uncertainties remain open, mainly due to the aspects related to the complexity of the soil-structure interaction phenomena [29,41]. Such a research topic is not completely covered by current standards, especially in presence of granular soils and in the case of structures characterized by the presence of more than two horizontal restrains. Furthermore, this work highlights that, for the design of underground structures, it is important to assess the response of the system taking into account the resonance effects between the seismic signal and the surrounding soil, which can significantly modify the dynamic response of the underground structure, and the geometrical system effects: these important aspects are not usually considered in current design approaches. As a consequence, the results obtained in this study can be considered useful also for the designers that should properly address the seismic design of shallow underground structures. On the other hand, considering current and recent important projects regarding shallow underground structures, the designers have primarily taken into account, at least in a first step, only the decoupled methods, also in presence of granular soils characterized by high values of shear waves velocity. For this reason, the authors have found it useful to perform a deep numerical insight into the limitations of such approaches in the seismic design of underground structures.

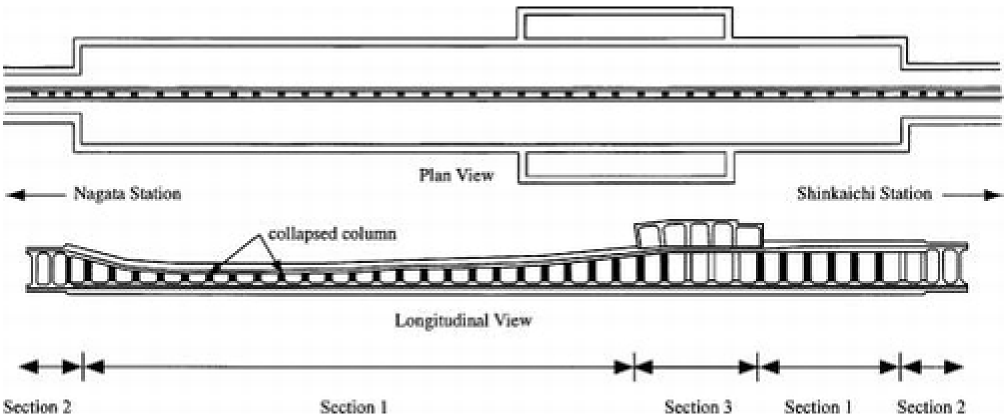

Fig. 1. Daikai metro station collapse [6].

2. SEISMIC DESIGN APPROACH FOR UNDERGROUND STRUCTURES

Underground structures are confined by the surrounding soil and cannot move separately; in fact, during an earthquake, they are affected by the deformations of the surrounding soil and by the inertial forces acting on the structures.

A proper seismic design should reduce the seismic vulnerability, providing structures with ability to resist the loads or limit the displacements generated by earthquakes. The main aim is to protect the human lives in the case of earthquakes and then to minimize economic losses. The design specifications should describe the ways for balancing structural strength with the intensity of the earthquakes that are likely to hit the structure. It is common in engineering practice to evaluate the static and the seismic response separately, but the final design involves both static and dynamic loads. In [3], the main steps for the analysis and seismic design of underground structures are described. In particular, four major steps are highlighted:

- seismic hazard assessment and selection of the design earthquake;
- evaluation of the transient soil response and induced phenomena;
- evaluation of the seismic behaviour of the structure;
- synthesis of seismic and static loads.

In order to define the seismicity of the area where the structure is located, it is possible to carry out a site-specific hazard analysis [40]. Once the outcrop motion has been defined, the characteristics of the ground motion at the depth of the structure may be obtained by different methods of soil response analysis. Usually, a deconvolution method is used to obtain the earthquake ground motion at the bedrock level, followed by a one-dimensional (1D) site response analysis in the case of simple soil stratification. The seismic ground motion is usually evaluated considering free-field conditions, without taking into account the presence of the structure. Another aspect of the design procedure is the evaluation of the structure behaviour under the expected soil shaking and the earthquake-induced deformations. It is possible to evaluate the transversal and the longitudinal contributions separately and, once the internal actions have been obtained, combine them later [11,17]. The internal actions obtained by the seismic analysis are combined with the results obtained by the static analysis to proceed to the final design of the underground structure [42].

In the last years, the numerical methods for the study of the soil-structure coupled system have had a strong development. For the evaluation of the seismic behaviour of underground structures, different types of numerical approaches are available nowadays. Depending on the complexity of the problem, it is possible to use 2D or 3D numerical models [18,25,43]. Usually, the seismic analysis is preceded by a construction stage analysis, taking into account all the main phases involved in the construction of the structure to reproduce the proper initial static conditions [32]. The seismic analysis is generally conducted through the non-linear time history analysis or 2D linear equivalent analysis, depending on the intensity of the seismic action.

3. SENSITIVITY ANALYSIS

The schematic sequence of the main phases of this study to investigate the seismic behaviour of a shallow multi-propped underground structures embedded in granular soils is shown in Fig. 2.

A sensitivity analysis has been performed considering the variation of the shear modulus (related to the shear wave velocity) of the homogeneous soil where the structure is embedded, Fig. 3. The model used is composed of 31.57 m soil profile overlying 51.30 m sandstone and the bedrock, Fig. 4.

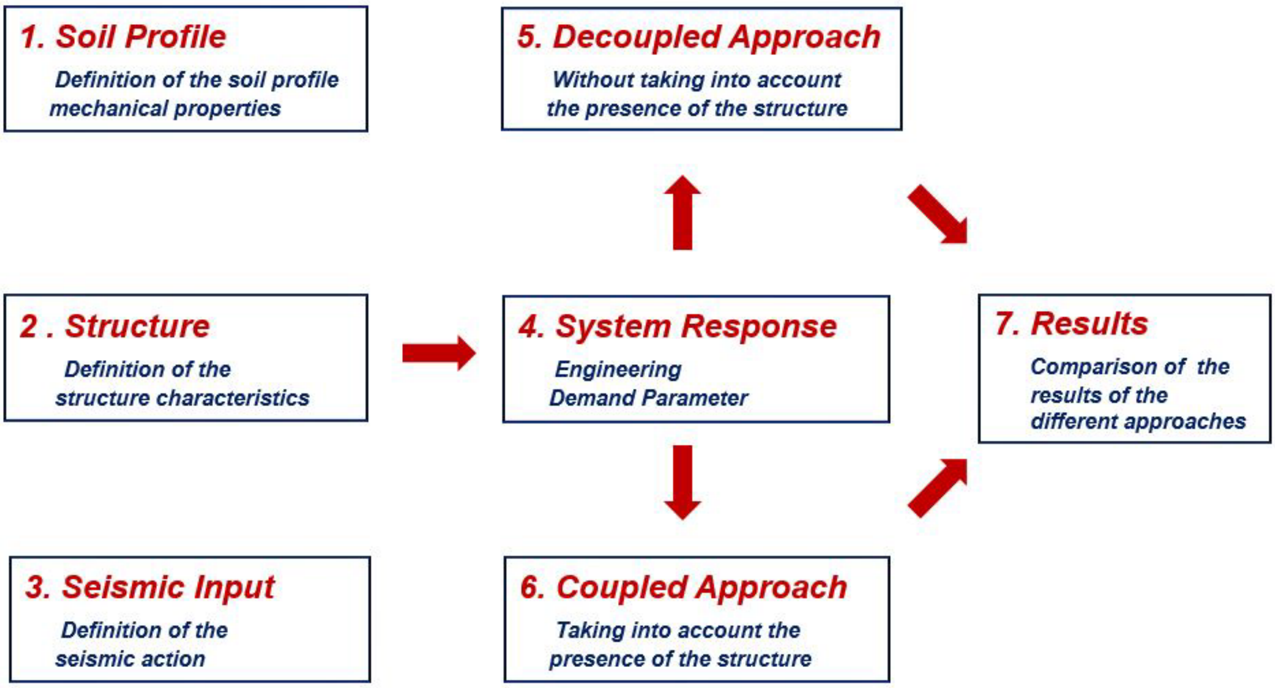

Fig. 2. Schematic sequence of the main phases of this study.

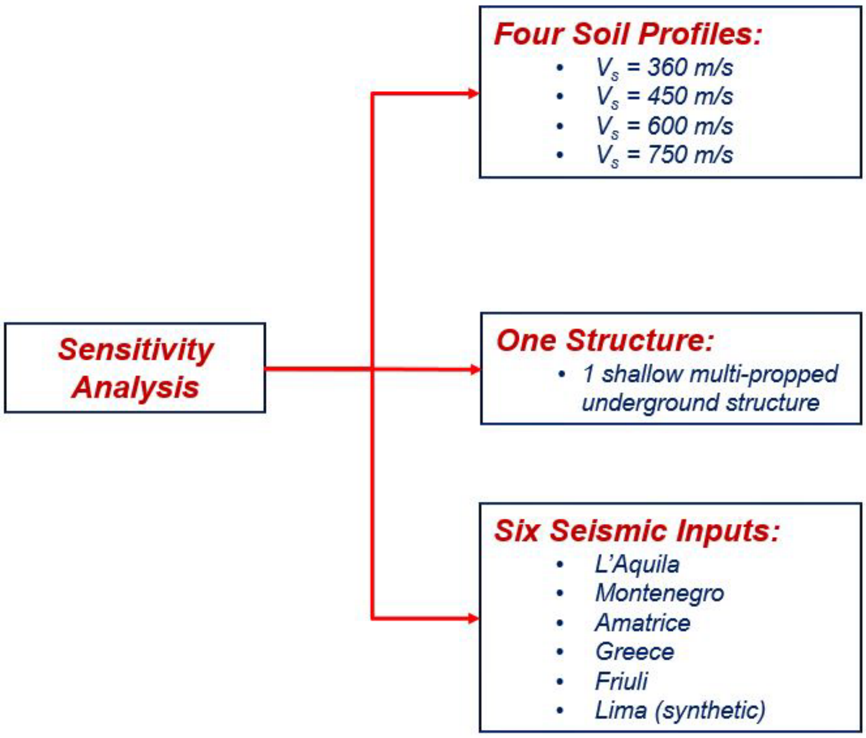

Fig. 3. Sensitivity analysis.

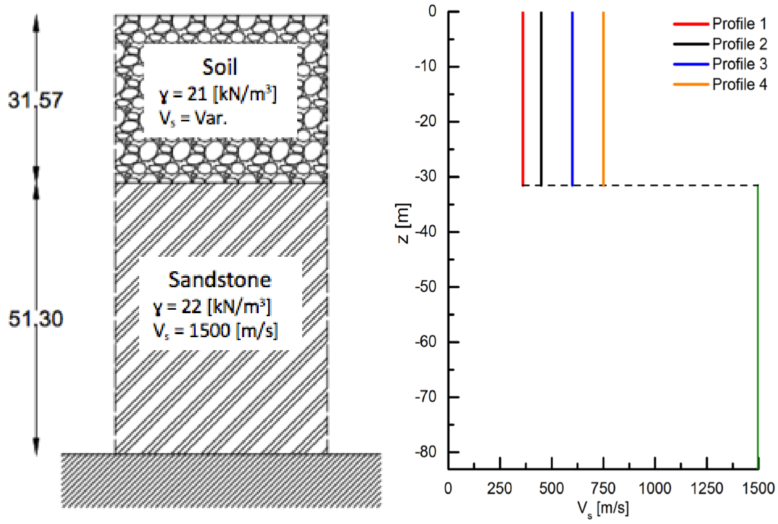

Fig. 4. Soil model and relative shear wave velocity profile.

Four different soil profiles, which are defined by a shear wave velocity ranging between 360 m/s and 800 m/s, have been chosen. Table 1 shows the main mechanical properties of the soil profiles considered in this study. The Poisson ratio (ν) is equal to 0.3 for all the soil profiles, while the dilatancy considered in this work is assumed equal to zero.

Table 1. Mechanical properties of the different soil profiles.

Soil Profile n°	Unit weight (γ) [kN/m^3]	Cohesion (c') [kPa]	Friction angle (φ') [°]	Shear wave velocity (V_S) [m/s]
1	21	40	39	360
2	21	40	39	450
3	21	40	39	600
4	21	40	39	750

The behaviour of underground structures under seismic actions is strictly related to the response of the surrounding soil to a given seismic input, in particular for the possible occurrence of resonance effects if the fundamental frequencies of the soil profile are close to the frequencies of the seismic input characterized by the maximum energy content. For this reason, five acceleration times histories recorded during different European seismic events (Greece, Amatrice, L'Aquila, Friuli and Montenegro), included within the European Strong-Motion Database, and one accelerogram generated analytically (considering the seismic characteristics of the city of Lima in Perù) for the metro station design, have been used. The main characteristics of the seismic inputs (PGA= peak ground acceleration, PGV = peak ground velocity, PGD = peak ground displacement) used in the sensitivity analysis are listed in Table 2.

Table 2. Characteristics of the seismic inputs used in the sensitivity analysis.

Event	**Event id**	**Station**	**Year**	**PGA**	**PGV**	**PGD**	**Magnitude (M_w)**	**Arias Intensity**
[-]	[-]	[-]	[-]	[g]	[cm/s]	[cm]	[-]	[cm/s]
Greece	GR-1995-0047	AIGA	1995	0.52	51.3	8.3	6.5	117.1
Amatrice	EMSC-20161030_0000029	AMT	2016	0.53	37.9	7.5	6.5	156.4
L'Aquila	IT-2009-0009	AQG	2009	0.49	35.8	6.0	6.1	132.4
Friuli	IT-1976-0030	FRC	1976	0.35	23.7	5.3	6	84.5
Montenegro	ME-1979-0003	PETO	1979	0.45	38.5	6.9	6.9	455.7
Lima	synthetic	-	2017	0.50	125.5	449.0	8.1	1492.0

The natural accelerograms have been chosen in order to have a Magnitude between 6 and 7 and a PGA value between 0.4 g and 0.6 g: however, they are characterized by different integral parameters values, gaining a large variability of the ground motion characteristics. The seismic signals have been applied both unscaled and scaled (only in terms of PGA, while keeping unchanged the frequency content of the seismic signals) considering a PGA value within 0.13 g and 0.22 g: it has to be mentioned that the scaled accelerograms have been used only for the evaluation of the system response. The signals and their form in the frequency domain, related to the fundamental natural frequencies of the soil columns evaluated according to [33], Table 3, are reported in Fig. 5 and Fig. 6, respectively.

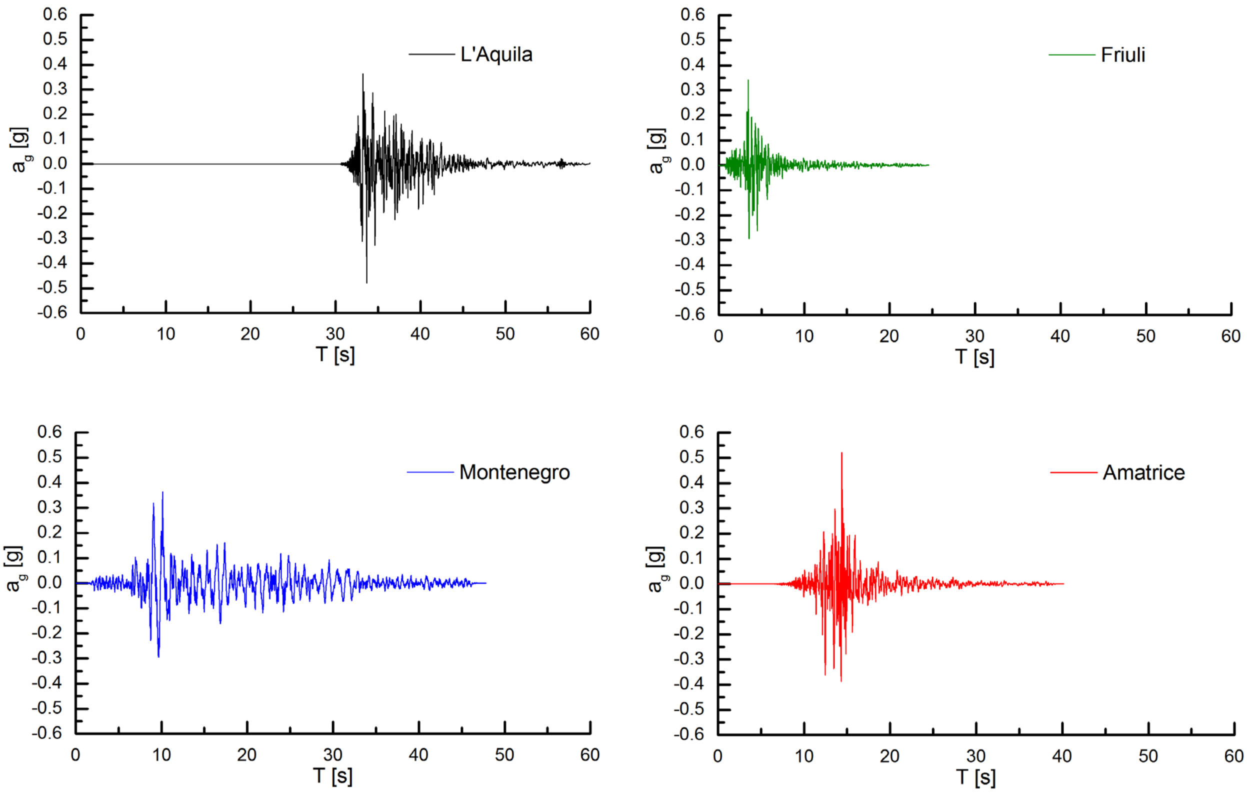

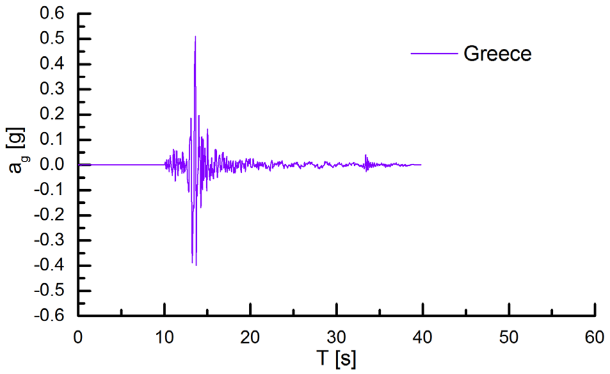

Fig. 5. Seismic inputs used in this study.

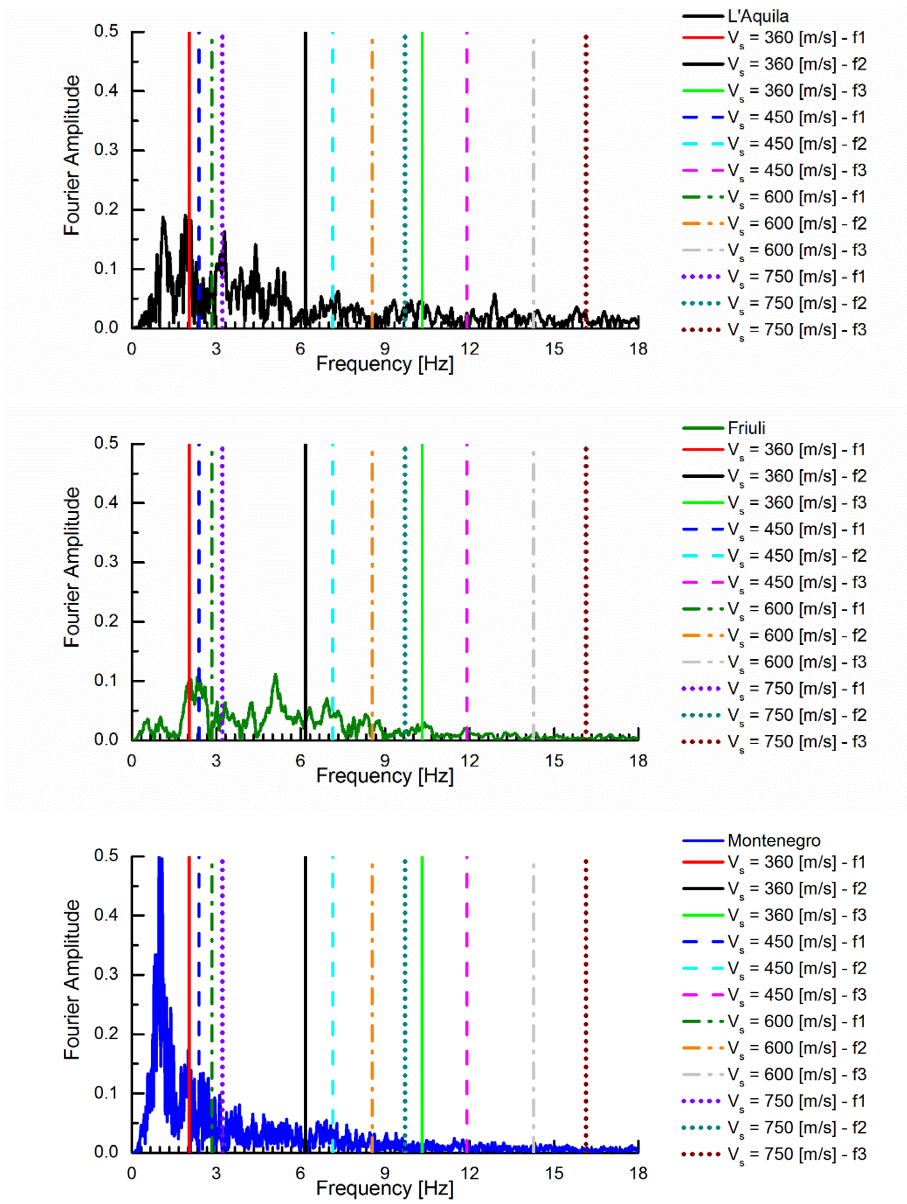

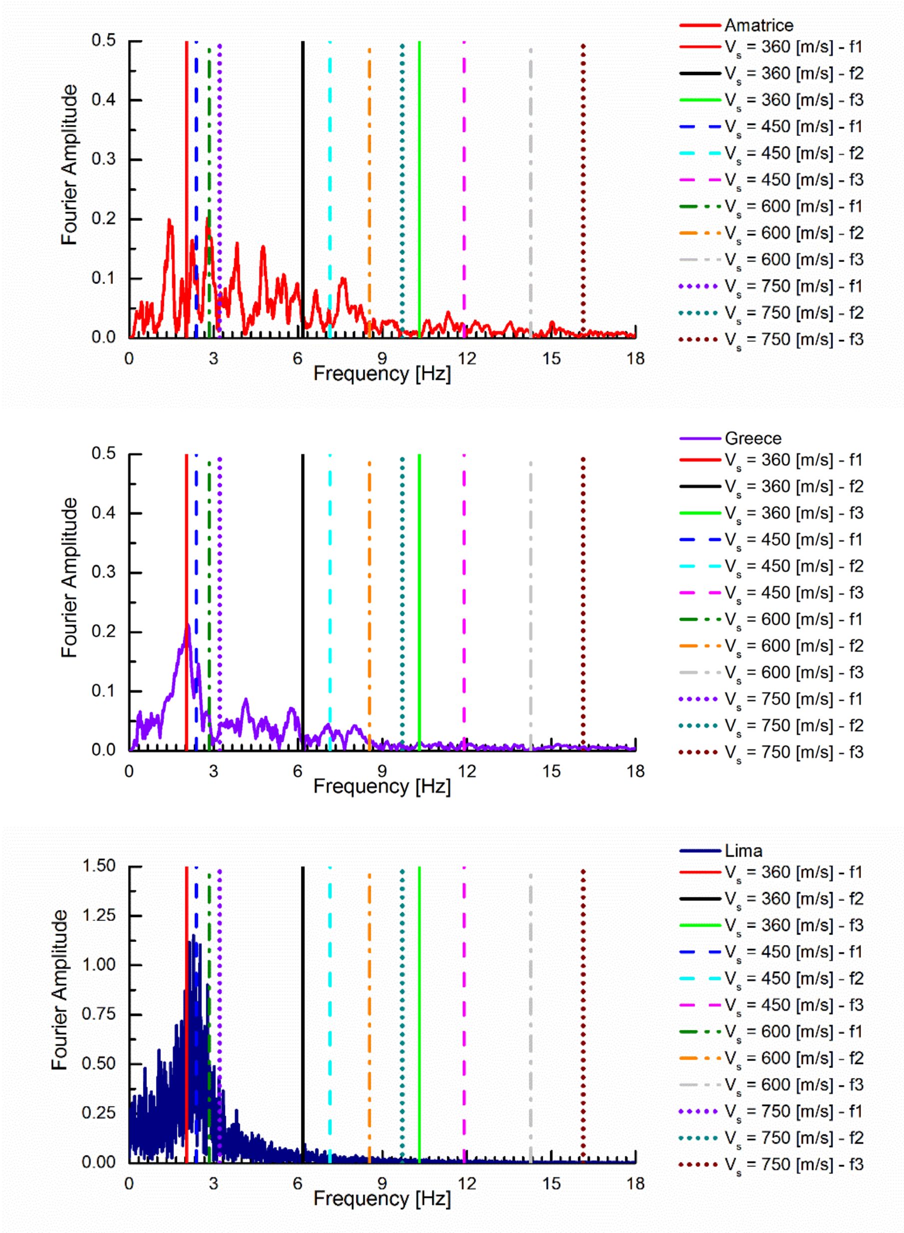

Fig. 6. Seismic signals in frequency domain.

Table 3. Soil profiles fundamental periods.

Soil profile V_S [m/s]	T_1 [s]	T_2 [s]	T_3 [s]
360	0.490	0.162	0.097
450	0.420	0.140	0.084
600	0.350	0.117	0.07
750	0.310	0.103	0.062

The relation between the frequency content of the seismic signals and the fundamental frequencies of the soil profiles is useful to understand the occurrence of possible resonance effects. The peaks of the Fourier transform of the different seismic inputs are localized near the frequencies range that includes the first fundamental frequency of the four soil profiles. Only for Montenegro seismic input, all the main peaks are found at lower frequencies compared to the first fundamental frequency characterizing the different soil profiles.

The structure considered in this study is characterized by a rectangular plan with dimensions equal to 132.16 m × 29.00 m, Fig. 7. The main structural elements are the RC retaining walls, which are 1 m thick, and a series of circular RC columns, which present a diameter equal to 1.2 m and are arranged according to a regular grid of 14.70 × 12.00 m. The foundations of the columns consist of circular RC piles, which present a diameter equal to 1.8 m and are 9 m deep. Fig. 8 shows the section of the RC retaining walls characterized by ϕ26 longitudinal rebars with a spacing equal to 15 cm (the yield moment is equal to about 2425 kNm).

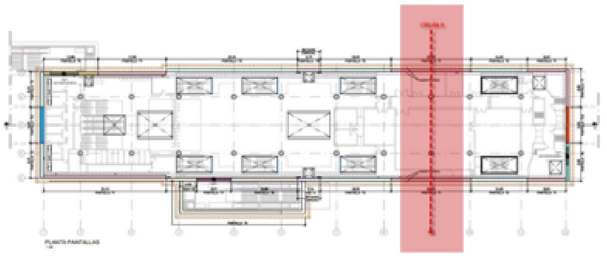

Structural Elements	Concrete (f_{ck}) [MPa]	Steel (f_{yk}) [MPa]
Columns	40	420
Piles	40	420
Retaining Walls	30	420
Slabs	40	420
	30	420

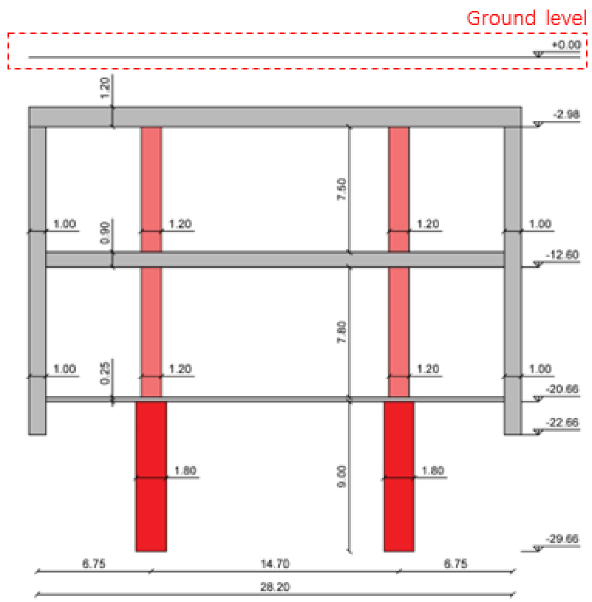

Fig. 7. The metro station (dimensions in meters).

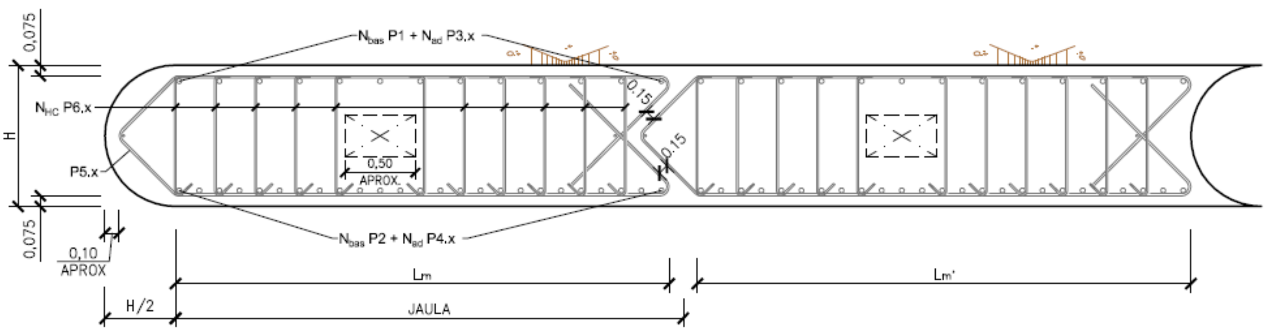

Fig. 8. Section of the RC retaining walls.

4. *NUMERICAL MODELLING*

The dynamic analyses have been performed, under plane strain conditions, through the finite difference code FLAC^{2D} [34]. The numerical model and the relative computation grid are shown in Fig. 9. An elastic perfectly plastic model with Mohr Coulomb strength rule for the soil, characterized by the mechanical properties listed in Table 1, has been adopted: a simple elastic constitutive law has been chosen for the sandstone. The shear stiffness at small strain, G_0, has been computed as a function of the shear wave velocity.

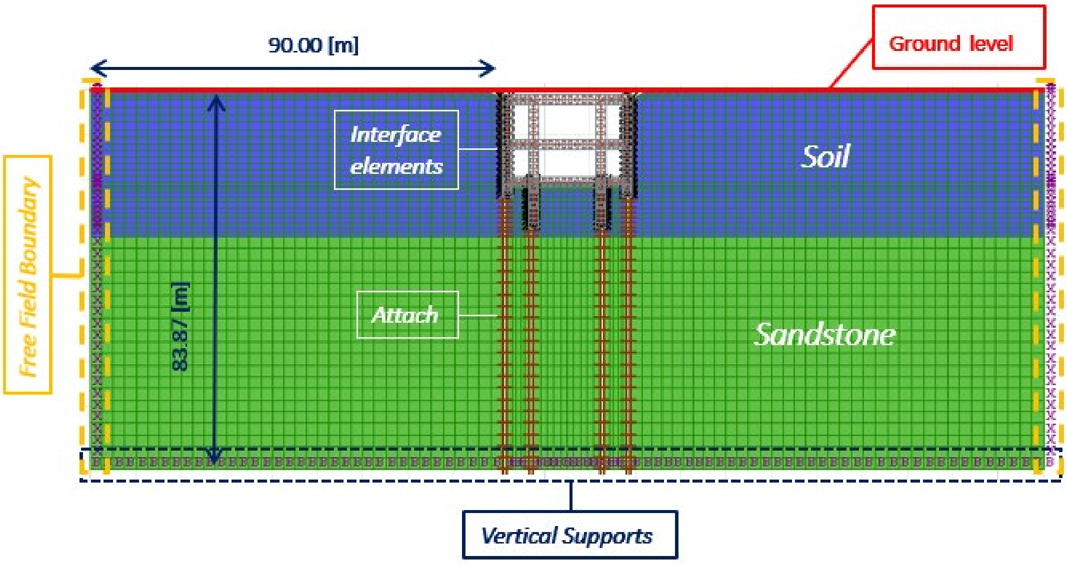

Fig. 9. Model geometry and computation grid for 2D analysis.

The maximum size of the computation mesh elements has been selected to allow the proper propagation of harmonics with 18 Hz frequency, which is the maximum frequency of the seismic inputs used in the sensitivity analysis, according to [35]. The formulation to optimize the size of the mesh is given in [36]. To minimize the reflection effects on the vertical lateral boundaries of the grid, free field boundary conditions available in FLAC 7.0 library have been used. The soil hysteretic behaviour has been modeled using the shear modulus decay curves given in [37,38]. As regards the hysteretic damping, the code FLAC uses the generalized Masing rules. The structure consists of linear elastic beam elements [43]: it is worth mentioning that the values of bending moment acting on the RC retaining walls obtained from all the approaches employed in this study are smaller than the yield moment (2425 kNm) of the RC retaining walls sections. Furthermore, the contact between soil and walls has been modelled by using elastic-perfectly plastic interface elements, with a friction angle equal to 20°. The values of the stiffness of the interface elements are evaluated according to the expressions reported in [34].
For the dynamic analyses, the selected acceleration time histories have been applied at the base of the computational grid considering the sandstone layer characterized by a damping equal to 1%.

5. *SEISMIC RESPONSE OF THE SYSTEM*

As highlighted in [18], the ground motion response obtained from the sensitivity analysis is significantly influenced by different overlapping effects:

1. different characteristics of the soil columns;
2. non-linear behaviour of the soil;
3. geometry of the system (2D effects);
4. soil-structure interaction effects.

The comparison between the parameters of the seismic inputs and those obtained at ground level allows for an evaluation of the magnitude of the seismic action in relation to the first two effects mentioned above.

The results of the free field analysis (i.e. in 1D condition for the scheme considered in this study), in terms of acceleration ratio (ratio of maximum acceleration at ground level, $PGA_{S\text{-}1D}$, to maximum acceleration of the seismic input, PGA), are shown for each soil profile in Fig. 10.

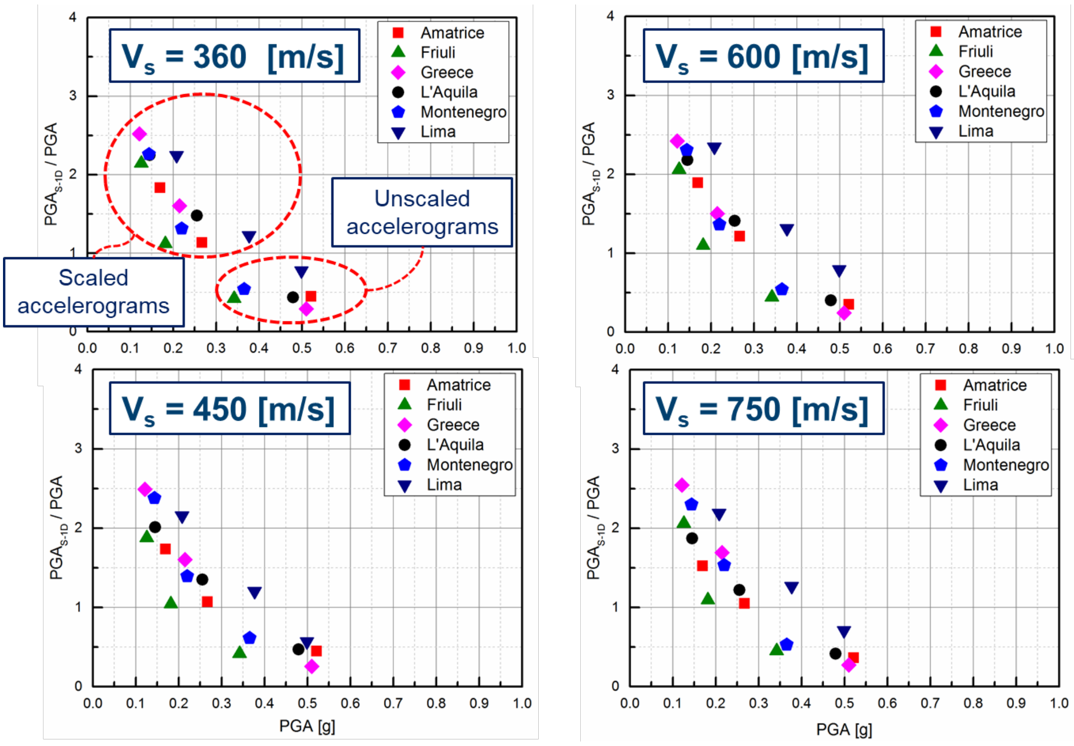

Fig. 10. 1D response factor.

The soil response, for the different seismic inputs, is related to the system vibration modes excited by the signal. In fact, the seismic response of the soil column is significantly influenced by the soil motion and straining due to the markedly non-linear behaviour of the soil.
The resonance effects with the first vibration mode of the different soil profiles lead to an increase of the shear strain in the deeper soil layers and, consequently, additional damping according to the strongly non-linear behaviour of the soil.
For these reasons, the free field analysis shows larger amplifications of the peak acceleration. Only for the unscaled accelerograms, the free field analysis shows a deamplification of the peak acceleration due to the characteristics of the seismic inputs that enhance the dissipation effects because of the non-linear behaviour of the soil.
The above-mentioned effects 3 and 4 are evaluated considering the ratio between the peak acceleration at the 2D model surface, $PGA_{S\text{-}2D}$, and the peak acceleration at the surface obtained in free field conditions, $PGA_{S\text{-}1D}$. The 2D effects and the structure embedded in the soil column generate an amplification of the seismic motion behind the walls and at the centre of the excavation for the focusing phenomena of the waves and seismic motion attenuation in front of the RC retaining walls due to the diffraction phenomena of the waves. Only for Lima seismic input, it is possible to observe a seismic motion attenuation in the centre of the excavation, as well as a greater amplification of the seismic action behind the walls when compared with the other seismic inputs, Fig. 11.

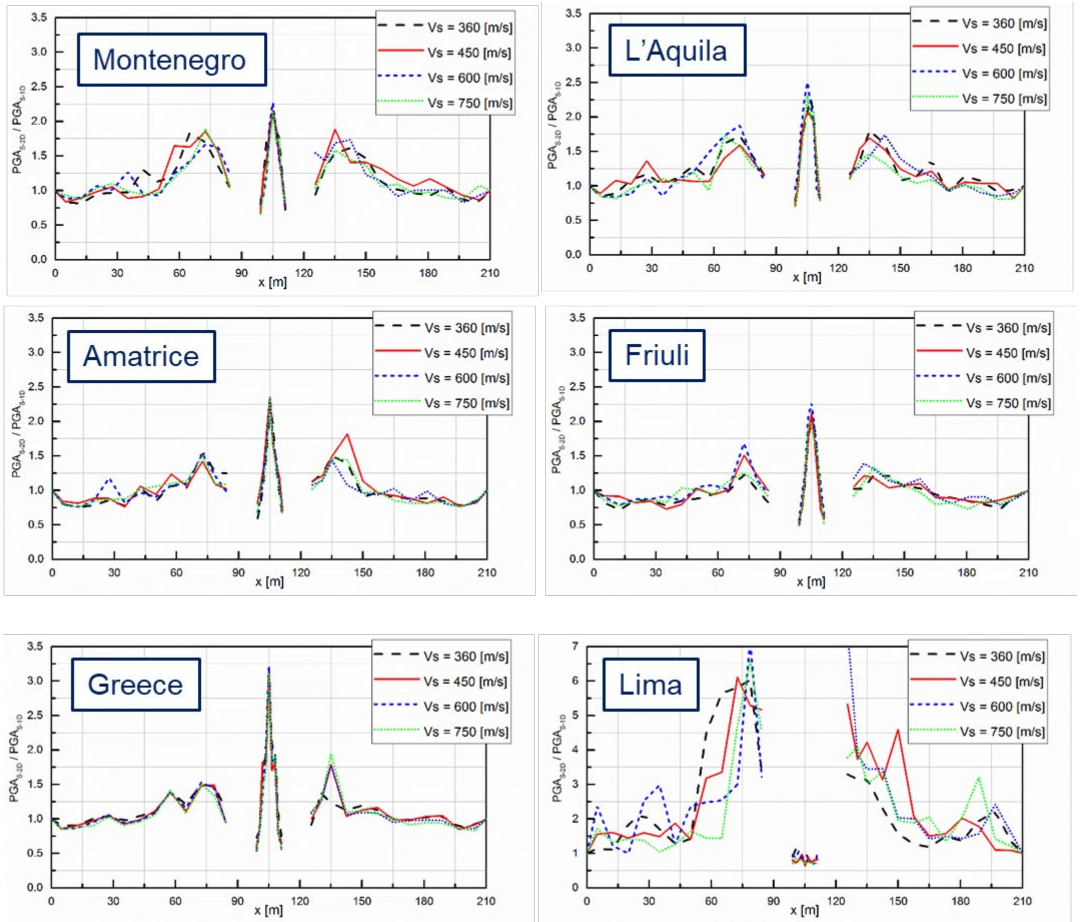

Fig. 11. 2D response factor.

The high stiffness of the structure causes additional reflections for the soil-structure interaction effects. The interaction of the reflected and incident wave fields modifies the shaking amplitude that depends on the phase shift of the two signals. The geometrical amplification and the phase shift are closely related to the frequency content of the signal that changes due to the non-linear behaviour of the soil.

6. *DECOUPLED APPROACH*

The decoupled approach considered in this study consists in the evaluation of the soil deformations without taking into account the presence of the structure (i.e. in free field conditions) and in the application of such deformations (evaluated at the depth of the structure) to the structure, according to the scheme reported in Fig. 12.

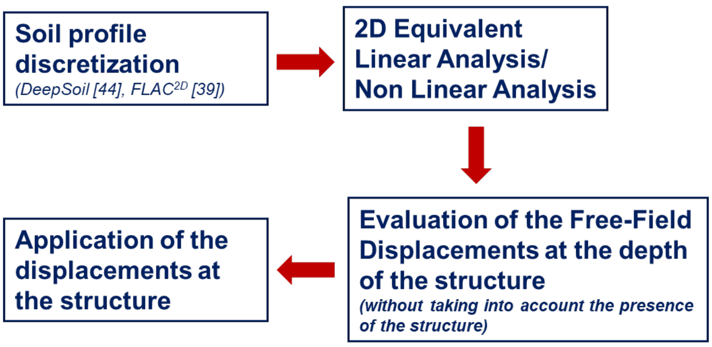

Fig. 12. Decoupled approach.

To simulate numerically the seismic response of the soil profiles and, consequently, obtain the displacements at both the top and the base of the structure, two different types of approaches have been used. The first method consists in the soil profiles discretization through the software code Deepsoil [39] and in the execution of an equivalent linear analysis. Also in such a case the degradation of the soil shear modulus has been modelled considering the decay curves given in [37]. Fig. 13 shows an example of the displacements distribution obtained for the soil profile characterized by a shear wave velocity V_S = 360 m/s under Montenegro seismic input (the solid line indicates the displacements profile starting from the depth of the structure base).

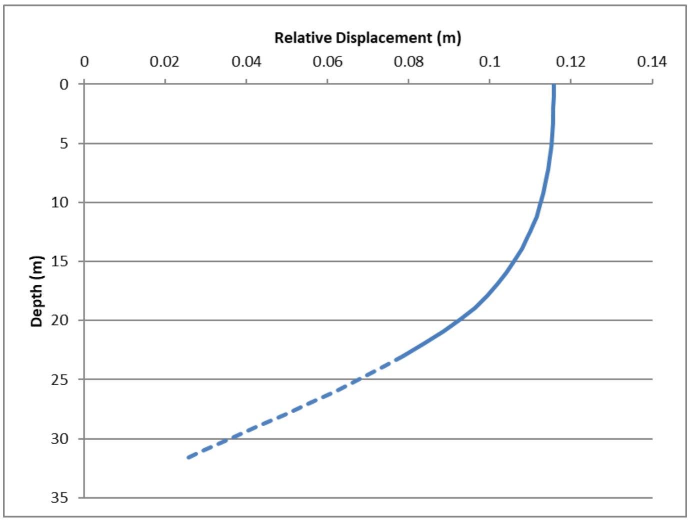

Fig. 13. Displacements distribution of the soil profile characterized by V_S = 360 m/s under Montenegro seismic input.

The displacements obtained for the other soil profiles subjected to different seismic inputs have shown a similar trend, resulting from the first vibration mode shape of the soil columns. These results are in accordance with the considerations expressed in Section 3, i.e. the seismic signals mainly excite the fundamental frequency of the soil profiles.

It is possible to note that the displacements evaluated at the ground level significantly decrease when the stiffness of the soil column increases.

Table 4 shows a synthesis of the results of the equivalent linear analysis, considering the values of the relative displacements obtained from the difference between the displacement evaluated at the depth corresponding to the top of the RC retaining walls of the underground structure and the displacement evaluated at the depth corresponding to the base of the RC retaining walls.

Table 4. Relative displacements obtained from the equivalent linear analysis.

	Relative Displacement					
SOIL PROFILE V_S	AMATRICE	FRIULI	GREECE	MONTENEGRO	L'AQUILA	LIMA
[m/s]	[mm]	[mm]	[mm]	[mm]	[mm]	[mm]
360	13	8	28	37	15	34
450	11	5	27	7	8	23
600	5	2	3	2	2	6
750	2	2	1	1	2	1

Taking into account the static case, the maximum increment of bending moment due to the seismic action is obtained: it can be noted that the maximum increase is registered for the soil profile characterized by a shear wave velocity equal to 360 m/s. In particular, the results of the equivalent linear analysis indicate that the maximum increase of bending moment is equal to 110 kNm in the case of Montenegro seismic input, while the bending moment increase due to the seismic action is almost negligible in the cases of soil profiles characterized by high values of stiffness (V_S = 600 m/s and V_S = 750 m/s).

In any case, the results show that the maximum value of bending moment acting on the RC retaining walls occurs in the section in correspondence with the central slab. Table 5 summarizes the main results, in terms of bending moment acting on such a section, obtained for the four different soil profiles.

Table 5. Bending moment acting on the section in correspondence with the central slab.

V_S [m/s]		*Montenegro*	*L'Aquila*	*Greece*	*Friuli*	*Amatrice*	*Lima*
360	Static (M_0) [kNm]	518	518	518	518	518	518
	Seismic (M) [kNm]	628	562	601	542	557	619
	Δ [%]	**21**	**9**	**16**	**5**	**7**	**20**
450	Static (M_0) [kNm]	451	451	451	451	451	451
	Seismic (M) [kNm]	472	475	532	466	484	520
	Δ [%]	**5**	**5**	**18**	**3**	**7**	**15**
600	Static (M_0) [kNm]	370	370	370	370	370	370
	Seismic (M) [kNm]	376	376	379	376	385	387
	Δ [%]	**2**	**2**	**2**	**2**	**4**	**5**
750	Static (M_0) [kNm]	312	312	312	312	312	312
	Seismic (M) [kNm]	315	318	315	318	318	315
	Δ [%]	**1**	**2**	**1**	**2**	**2**	**1**

For the second method, the free-field displacements obtained from the numerical model described in Section 4 through the non-linear dynamic analysis have been used. Table 6 summarizes the main results of the non-linear analysis in terms of relative displacements.

Table 6: Relative displacements obtained from the non-linear analysis.

	Relative Displacement					
SOIL PROFILE V_s	AMATRICE	FRIULI	GREECE	MONTENEGRO	L'AQUILA	LIMA
[m/s]	[mm]	[mm]	[mm]	[mm]	[mm]	[mm]
360	18	12	33	42	19	120
450	16	8	30	13	10	107
600	8	4	7	4	4	36
750	5	3	2	2	4	23

Also for the second approach, the maximum increment of bending moment due to seismic action occurs in the soil profile characterized by low values of shear wave velocity and the maximum increase of bending moment is equal to 357 kNm in the case of Lima seismic input. Table 7 summarizes the main results in terms of bending moment acting on the section in correspondence with the central slab.

Table 7. Bending moment acting on the section in correspondence with the central slab.

V_S [m/s]		*Montenegro*	*L'Aquila*	*Greece*	*Friuli*	*Amatrice*	*Lima*
360	Static (M_0) [kNm]	518	518	518	518	518	518
	Seismic (M) [kNm]	643	574	616	554	571	875
	Δ [%]	**24**	**11**	**19**	**7**	**10**	**69**
450	Static (M_0) [kNm]	451	451	451	451	451	451
	Seismic (M) [kNm]	490	481	541	475	499	769
	Δ [%]	**9**	**7**	**20**	**5**	**11**	**71**
600	Static (M_0) [kNm]	370	370	370	370	370	370
	Seismic (M) [kNm]	382	384	390	382	393	477
	Δ [%]	**3**	**4**	**6**	**3**	**6**	**29**
750	Static (M_0) [kNm]	312	312	312	312	312	312
	Seismic (M) [kNm]	315	327	318	321	327	381
	Δ [%]	**1**	**5**	**2**	**3**	**5**	**22**

The comparison of the results of the two different methods has shown that the relative displacements obtained by the non-linear analysis are greater than those obtained by the equivalent linear analysis. Consequently, also the increase of the bending moment acting on the RC retaining walls follows this trend, Table 8.

Table 8. Comparison of the results in terms of bending moment acting on the section in correspondence with the central slab.

V_S [m/s]		*Montenegro*	*L'Aquila*	*Greece*	*Friuli*	*Amatrice*	*Lima*
360	EL [kNm]	628	562	601	542	557	619
	NL [kNm]	643	574	616	554	571	875
	Δ [%]	**2**	**2**	**2**	**2**	**3**	**41**
450	EL [kNm]	472	475	532	466	484	520
	NL [kNm]	490	481	541	475	499	769
	Δ [%]	**4**	**1**	**2**	**2**	**3**	**48**
600	EL [kNm]	376	376	379	376	385	387
	NL [kNm]	382	384	390	382	393	477
	Δ [%]	**2**	**2**	**3**	**2**	**2**	**23**
750	EL [kNm]	315	318	315	318	318	315
	NL [kNm]	315	327	318	321	327	381
	Δ [%]	**0**	**3**	**1**	**1**	**3**	**21**

The results show that the difference (Δ) of the values of bending moment acting on the section in correspondence with the central slab obtained through the non-linear analysis (NL) and those obtained through the equivalent linear analysis (EL) lies between 2% and 4% for all the natural accelerograms. Such a limited value is due to the incidence of the bending moment obtained under static conditions on the final bending moment compared to the increment due to the seismic action. The same situation does not occur for Lima accelerogram: in such a case, the difference is greater than 40% for the soil profiles characterized by V_S = 360 m/s and 450 m/s, and almost equal to 20% for the soil profiles characterized by V_S = 600 m/s and 750 m/s. This difference is due to the particular characteristics of Lima seismic input (see Table 2, Fig. 5 and Fig. 6) when compared with the other natural accelerograms considered in this work.

7. COUPLED APPROACH

The coupled approach is performed through the numerical model described in detail in Section 4.
In the static phase, the boundary conditions and the loads considered are the following:

- vertical supports at the base nodes to restrain vertical displacements;
- horizontal supports at the lateral nodes to permit vertical soil settlements;
- dead loads equal to 50 kN/m^2 (due to the presence of existing buildings and streets) that are applied on the sides of the station;
- dead loads equal to 20 kN/m^2 (due to the presence of streets) that are applied in correspondence with the station;
- self-weight of the structure and soil.

The static condition is determined by performing a construction stage analysis. The sequence of the construction phases is summarized as follows:

- the realization of an excavation, characterized by a provisional slope 1H : 5V to create a first entrance ramp;
- the realization of the vertical structural elements of the underground structure;
- the realization of the top cover RC slab that is 1.2 m thick;
- the execution of a second excavation until a depth equal to 12.60 m;
- the realization of the intermediate RC slab that is 0.9 m thick;
- the execution of a third excavation until a depth equal to 20.66 m;
- the realization of the bottom RC slab that is 0.25 m thick;
- the road surface restoration.

After the last step of the construction stage analysis, a non-linear dynamic time-history analysis has been performed, considering the different types of soil profiles and the set of six seismic inputs. During the main shaking stage, the loads distribution on the RC retaining walls appears slightly asymmetric, while at the end of the seismic event (residual moment) it tends to balance: i.e Fig. 14 shows the results in terms of maximum bending moment during the seismic excitation (black line), residual bending moment at the end of the seismic excitation (red line) and initial bending moment (blue line), for the soil profile characterized by V_S = 360 m/s under Montenegro seismic input. Such a consideration is valid only for the five natural accelerograms, because in the case of Lima seismic input the loads distribution on the RC retaining walls remains asymmetric also at the end of the seismic event, Fig. 15.
Table 9 summarizes the main results in terms of maximum bending moment occurred during the seismic analyses on the section in correspondence with the central slab. For all the accelerograms, the increment due to the seismic action is higher for the soil profiles characterized by V_S = 600 m/s and 750 m/s, in contrast with the decoupled approach results.

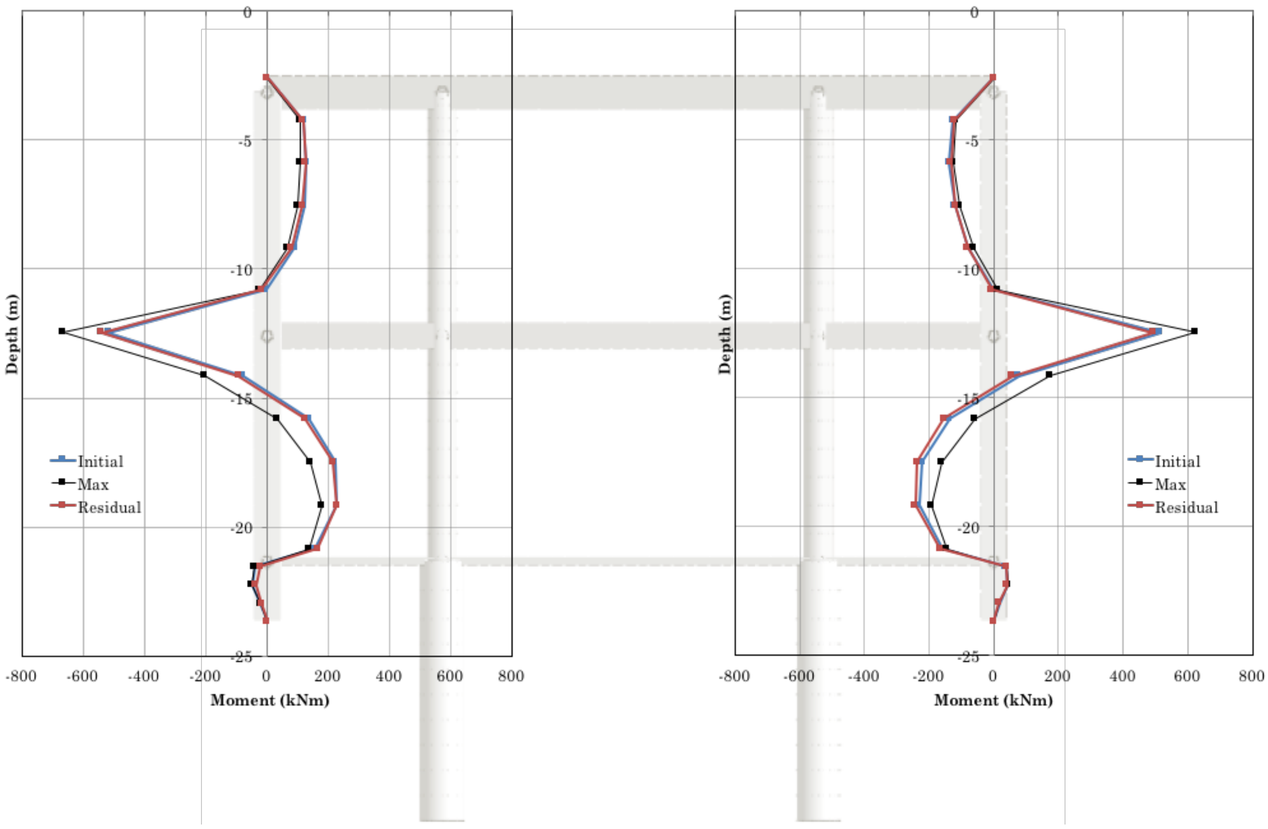

Fig. 14. Bending moment acting on the RC retaining walls in the case of soil profile characterized by Vs = 360 m/s and Montenegro seismic input.

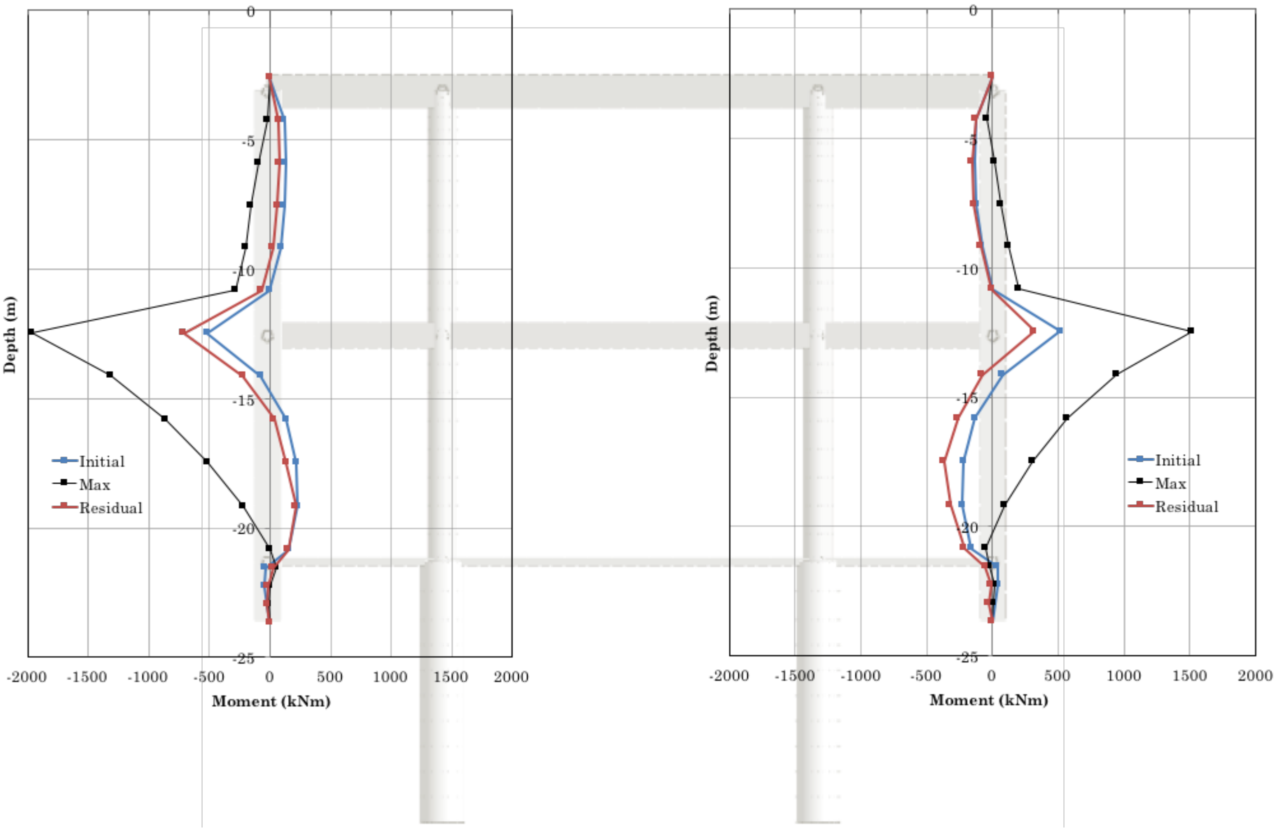

Fig. 15. Bending moment acting on the RC retaining walls in the case of soil profile characterized by Vs = 360 m/s and Lima seismic input.

Table 9. Bending moment acting on the section in correspondence with the central slab.

V_S [m/s]		*Montenegro*	*L'Aquila*	*Greece*	*Friuli*	*Amatrice*	*Lima*
360	Static (M_0) [kNm]	518	518	518	518	518	518
	Seismic (M) [kNm]	665	659	652	639	647	1967
	Δ [%]	**28**	**27**	**26**	**23**	**25**	**279**
450	Static (M_0) [kNm]	451	451	451	451	451	451
	Seismic (M) [kNm]	600	589	593	579	587	1977
	Δ [%]	**33**	**31**	**31**	**28**	**30**	**338**
600	Static (M_0) [kNm]	370	370	370	370	370	370
	Seismic (M) [kNm]	518	506	513	500	504	1890
	Δ [%]	**40**	**37**	**37**	**35**	**36**	**411**
750	Static (M_0) [kNm]	312	312	312	312	312	312
	Seismic (M) [kNm]	458	451	454	438	447	1805
	Δ [%]	**47**	**45**	**46**	**40**	**43**	**479**

8. COMPARISON OF THE RESULTS

As mentioned before, the displacements obtained through the decoupled approach considering the equivalent linear analysis follow a trend resulting from the first vibration mode shape of the soil columns. According to Fig. 5, in fact, the seismic signals mainly excite the fundamental frequency of the soil profiles. Moreover, the displacement evaluated at the ground level significantly decreases when the stiffness of the soil column increases.
The results of the equivalent linear analysis indicate that the maximum increase of bending moment is equal to 110 kNm under Montenegro seismic input, while it is possible to observe that the bending moment increase due to the seismic action is almost negligible in the cases of soil profiles characterized by shear wave velocities equal to V_S = 600 m/s and V_S = 750 m/s.
The maximum increment of bending moment (equal to 357 kNm) occurs in the soil profile characterized by V_S = 360 m/s for Lima seismic input, always taking into account the decoupled approach but considering the results obtained from the 1D non-linear dynamic analysis.
The difference of the results, in terms of bending moment acting on the section in correspondence with the central slab, obtained through the equivalent linear analysis and those obtained through the non-linear analysis ranges from 2% to 4% for all the natural accelerograms. Such limited values are due to the incidence of the value of the bending moment obtained under static conditions on the value of the final bending moment compared to the increment due to the seismic action. The same situation does not occur for Lima synthetic signal: the difference between the results is significant (greater than 40% for the soil profiles characterized by V_S = 360 m/s and 450 m/s, and almost equal to 20% for the soil profiles characterized by V_S = 600 m/s and 750 m/s).
The results of the coupled approach have shown that for all the accelerograms the increment due to the seismic action is higher for the soil profiles characterized by Vs = 600 m/s and 750 m/s, in contrast with the decoupled approach results. The maximum increment, also in this case, occurs under Lima seismic signal and is equal to 1493 kNm for the soil profile characterized by V_S = 750 m/s. On the other hand, for the natural accelerograms, the maximum increment obtained is equal to about 150 kNm, always under Montenegro seismic input. The trend of the maximum value of the bending moment, obtained during the seismic event, acting on the section in correspondence with the central slab has shown a decrease of the maximum value when the soil column stiffness increases.
Fig. 16 compares the results of the decoupled and coupled approaches in terms of the ratio between the maximum value of bending moment in correspondence with the central slab section obtained

during the seismic event (M) and the value of the initial static moment (M_0). Such ratios obtained through the coupled approach are always larger than those obtained through the decoupled approach. It can be noted that the differences are greater for the synthetic accelerogram (Lima): the decoupled approach appears to underestimate the internal actions on the structural elements. For the other seismic inputs, the differences are moderate for the soil profiles characterized by low values of stiffness, confirming the validity of the approach, but tend to increase for the soil profiles characterized by V_S larger than 450 m/s.

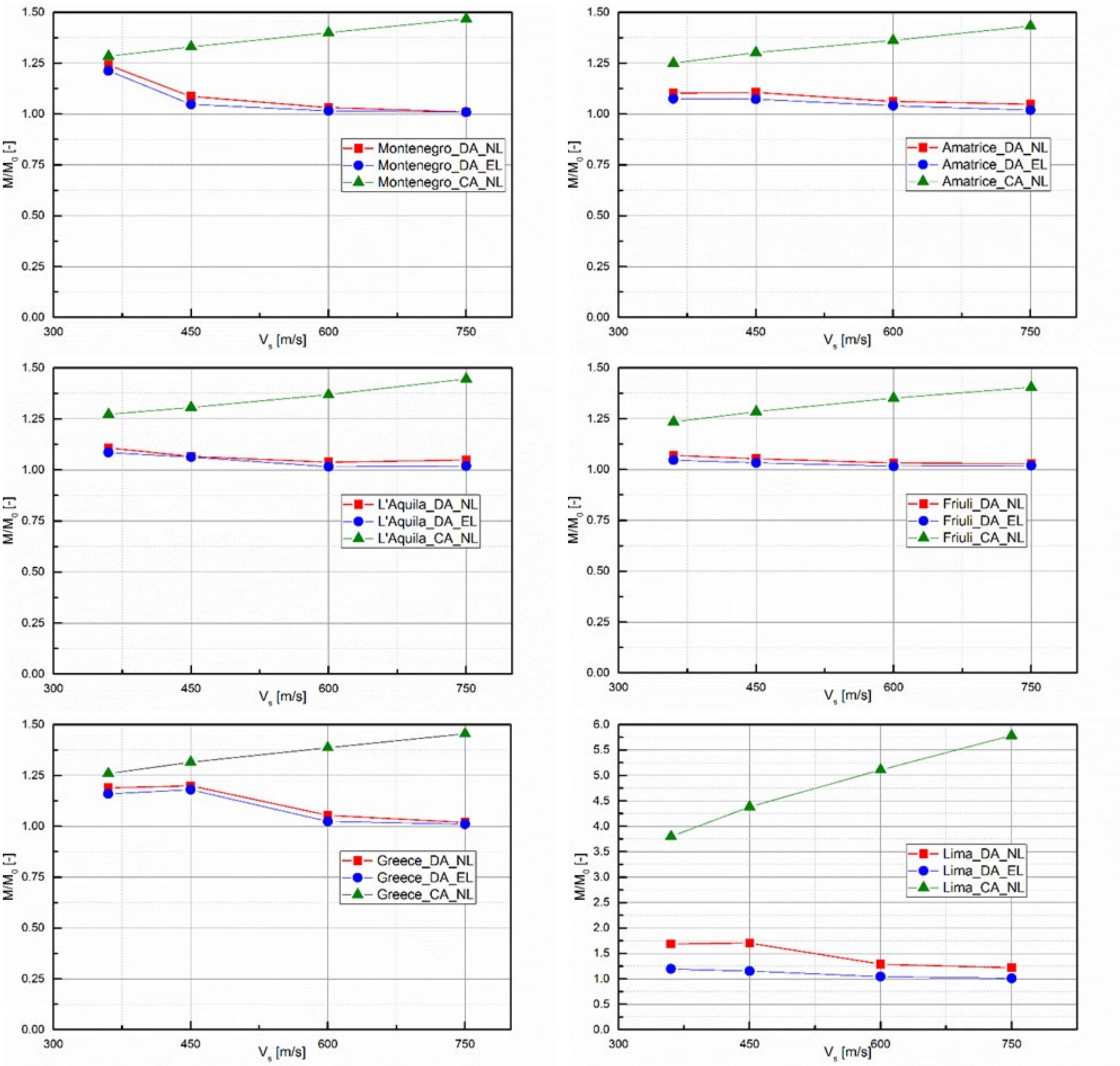

Fig. 16. Comparison of the results (M = maximum value of bending moment registered during the seismic excitation; M_0 = initial static moment).

9. *CONCLUSIONS*

This paper has investigated the seismic behaviour of a shallow multi-propped underground structure (metro station) embedded in granular soils through a large set of numerical simulations. The sensitivity analysis carried out on the underground structure has involved six seismic signals and four

different soil profiles, which are characterized by the same mechanical properties but different values of the shear modulus related to the shear wave velocity ranging between 360 m/s and 750 m/s. A decoupled approach has been adopted and two different types of analyses (an equivalent linear analysis using the software code Deepsoil and a non-linear dynamic analysis using the numerical model described in Section 4 have been conducted in order to obtain the soil column displacements at the depth of both the top and the base of the structure, without taking into account the presence of the structure. The results obtained have been compared with those obtained through the coupled approach performing a non-linear dynamic analysis implemented in the software code Flac^{2D}.
The numerical investigations conducted in this study have shown that the decoupled approach, which requires a significantly lower computational effort than the coupled approach, provides consistent results only for soil profiles characterized by low values of stiffness (V_S < 450 m/s), because it is strictly related to the displacements distribution along the soil column, and for seismic signals characterized by limited values of Arias Intensity. Such results indicate some limitations concerning its application that are mainly due to the following assumptions underlying the approach: i) the criterion of the simultaneity of the actions on the structural elements is not considered because only the maximum values of the displacements recorded during the seismic events are taken into account; ii) the resonance effects between the structure and the soil column are not taken into account; iii) the modifications of the seismic signal at the ground level due to the presence of the structure are not taken into account. Moreover, it is worth mentioning that the trend of the displacements along the soil column strictly depends on the non-linear behaviour of the soil and how it is implemented in the approach (equivalent linear analysis or non-linear analysis): in any case, the influence on the final results in terms of structural design seems to be marginal for the high incidence of the internal action obtained under static conditions on the structural elements. Furthermore, the values of bending moment acting on the RC retaining walls obtained from all the approaches previously described are smaller than the yield moment (2425 kNm) of the RC retaining walls sections.
Finally, it is worth mentioning that the results obtained in this work are related to the specific geometrical features of the structure under study: more generalized results can be obtained considering different types of structural configurations and using a nonlinear constitutive model for the beam elements, as reported in [44,45].

References

[1] Bickel JO. Tunnel engineering handbook; Chapman and Hall, New York, 1996.

[2] Power M, Rosidi D, Keneshiro J, Gilstrap S, Chiou SJ. Summary and evaluation procedures for the seismic design of tunnels. Final report task 112-d-5.3(c). Buffalo: National centre for earthquake engineering research, 1998.

[3] Hashash YMA, Hook J, Schmidt B, Yao J. Seismic design and analysis of underground structures. Tunnelling and Underground Space Technology;16: pp. 247-293, 2001.

[4] Gazetas G, Gerolymos N, Anastasopoulos I. Response of three Athens metro underground structure in the 1999 Parintha earthquake. Soil Dynamics and Earthquake Engineering 25: pp. 617-633, 2005.

[5] Iida H, Hiroto T, Yoshida N, Iwafuji M. Damage to Daikai subway station. In special issue on geotechnical aspects of January 17 1995 Hyogoken-Nanbu earthquake. Japan: Soil and Foundations 1996.

[6] Huo H, Bobet A, Fernandez G, Ramirez J. Load transfer mechanisms between underground structure and surrounding ground: evaluation of the failure of the Daikai station. Journal of Geotechnical and Geoenvironmental Engineering, Volume 131, Issue 12, December 2005.

[7] Wang JN Seismic Design of Tunnels; Parson Brinckerhoff Inc., New York, 1993.

[8] Penzien J. Seismically induced racking of tunnels lining. Earthquake Engineering and Structural Dynamics 27: pp. 683-691, 2000.

[9] JRA (Japan Road Association). Guide specifications of design and construction of underground parking lots. Tokyo: Ministry of Transportation, 1992.

[10] Kawashima K. Seismic analysis of underground structures. Journal of Disaster Research 1(3): pp. 378-389, 2006.

[11] ISO (International Organization for Standardization). ISO 23469: Bases for design of structures - Seismic actions for designing geotechnical works. International Standard ISO TC98/SC3/WG10. Geneva: International Organization for Standardization, 2005.

[12] Hoeg K. Stresses against underground structural cylinders. Journal of Soil Mechanics and Foundations Division, ASCE 94: pp. 833-858, 1968.

[13] Penzien J, Wu C. Stresses in linings of bored tunnels. Earthquake Engineering and Structural Dynamics 27: pp. 283-300, 1998.

[14] Bobet A. Effect of pore water pressure on tunnel support during static and seismic loading. Tunneling and Underground Space Technology, 18(4): pp. 377-393, 2003.

[15] Park KH, Tantayopin K, Tontavanich B, Owatsiriwong A. Analytical solution for seismic-induces ovaling of circular tunnel lining under no-slip interface conditions: A revisit. Tunneling and Underground Space Technology 24(2): pp. 231-235, 2009.

[16] Bobet A. Drained and undrained response of deep tunnels subjected to far-field shear loading. Tunneling and Underground Space Technology 25(1): pp. 21-31, 2010.

[17] FHWA (Federal Highway Administration). Technical manual for design and construction of road tunnels - Civil elements. Publication No. FHWA-NHI-10-034. Washington DC: Department of transportation, Federal Highway Administrator, 2009.

[18] Soccodato FM, Tropeano G. The role of ground motion characters on the dynamic performance of propped retaining structures. 6ICEGE, 6th International Conference on Earthquake Geotechnical Engineering, 1 – 4 November 2015, Christchurch, New Zealand, 2015.

[19] Zucca M, Tropeano G, Crespi P, Erbì E. 2D linear equivalent analysis for the seismic vulnerability evaluation of multi-propped retaining structures. XVII ECSMGE – European Conference on Soil Mechanics and Geotechnical Engineering, 1 – 6 September 2019, Reykjavik, Iceland, 2019.

[20] Newmark NM. Problems in wave propagation in soil and rock. In Proc. of international symposium on wave propagation and dynamic properties of earth materials. New Mexico: University of New Mexico Press, 1968.

[21] Kuesel E, Christian JT, Roesset JM. Nonlinear behaviour in soil-structure interaction. Journal of Geotechnical Engineering Division, ASCE 102(11): pp. 1159-1170, 1976.

[22] St. John CM, Zahrah TF. Aseismic design of underground structures. Tunneling and Underground Space Technology 2(2): pp. 165-197, 1987.

[23] Kiyomiya O. Earthquake-resistant design features of immersed tunnels in Japan. Tunneling and Underground Space Technology 10(4): 463-475, 1995.

[24] Gomez-Masso A, Attala I. Finite element vs. simplified methods in the seismic analysis of underground structures. Earthquake Engineering and Structural Dynamic, 12: pp. 347-367, 1984.

[25] Zucca M, Tropeano G, Erbì E, Crespi P. Evaluation of the seismic behaviour of multi-propped shallow underground structures embedded in granular soils: a comparison between coupled and decoupled approaches. 7ICEGE, 7th International Conference on Earthquake Geotechnical Engineering, 17 – 20 June 2019, Rome, Italy, 2019.

[26] Lanzano G, Bilotta E, Russo G. Tunnel under seismic loading: a review of damage case histories and protection methods. RELUIS Guidelines, 2012.

[27] Xie Y. Seismic response analysis method of underground structures in China. IFEESM 2015, International Forum on Energy, Environment Science and Materials, Shenzhen, China, 2015.

[28] Andreotti G, Lai CG. Methodology to Derive Damage State-Dependent Fragility Curves of Underground Tunnels. 6ICEGE, 6th International Conference on Earthquake Geotechnical Engineering, 1 – 4 November 2015, Christchurch, New Zealand, 2015.

[29] Pitilakis K, Tsinidis G. Recent advances on the seismic behaviour and design of tunnels. AGI conference, Catania, Italy, 2016.

[30] Pavlovic N. Ground response analysis as an essential part of earthquake-resistant structures design. Asia 2004, Conference on Earthquake Engineering, ASEP, Manila 2004.

[31] Kramer SL. Geotechnical Earthquake Engineering; Prentice-Hall, New Jersey, 1996.

[32] Zucca M, Crespi P, Longarini N. Seismic vulnerability assessment of an Italian historical masonry dry dock. Case Studies in Structural Engineering (7): pp. 1-23, 2017.

[33] Maugeri M, Carrubba P, Frenna SM. Frequenze e modi di vibrazione di terreni eterogenei. Associazione Geotecnica Italiana, 1988.

[34] Itasca Consulting Group Inc., 2007 FLAC^{2D}: Fast Legrangian Analysis of Continua.

[35] Kuhlemeyer R, Lysmer J. Finite element method accuracy for wave propagation problems. Journal of Soil Mechanics & Foundations Division. ASCE, 99(SM5): pp. 421-427, 1973.

[36] Pagliaroli A, Lanzo G, Sanò T. Confronto fra tre codici di calcolo 2D della risposta sismica locale. XII Congresso Nazionale "l'Ingegneria sismica in Italia", ANIDIS, 2007.

[37] Seed HB, Idriss IM. Soil moduli and damping factors for dynamic analysis. Report No. EERC 70-10, University of California, Berkeley, 1970.

[38] Stokoe KH, Jung MJ, Menq FY, Liao T, Massoudi N, McHood M. Normalized shear modulus of compacted gravel. 18th International Conference on Soil Mechanics and Geotechnical Engineering, Paris, France, 2013.

[39] Hashash YMA, Musgrove MI, Harmon JA, Groholski DR, Phillips CA, Park D. DEEPSOIL 6.1, User Manual. Urbana, IL, Board of Trustees of University of Illinois at Urbana-Champaign, 2016.

[40] Wang S, Li J, Luo H, Zhu H. Damage identification in underground tunnel structures with wavelet based residual force vector. Engineering Structures, Vol. 178, pp. 506-520, 2019.

[41] Lu L, Qiu J, Yuan Y, Tao J, Yu H, Wang H, Mang H. Large-scale tests as the basis of investigating the fire-resistance of underground RC substructures. Engineering Structures, Vol. 178, pp. 12-23, 2019.

[42] Nam SH, Song HW, Byun KJ, Maekawa K. Seismic analysis of underground reinforced concrete structures considering elasto-plastic interface elements with thickness. Engineering Structures, Vol 28 (8), pp. 1122-1131, 2006.

[43] Tropeano G, Soccodato FM. Dynamic analyses of propped retaining structures. In Proc. 8th European Conference on Numerical Methods in Geotechnical Engineering, NUMGE 2014, 2, pp. 1193-1198, 2014.

[44] Andreotti G, Lai CG. A nonlinear constitutive model for beam elements with cyclic degradation and damage assessment for advanced dynamic analyses of geotechnical problems. Part I: theoretical formulation. Bulletin of Earthquake Engineering 2017;15(7):2785-2801, 2017.

[45] Andreotti G, Lai CG. A nonlinear constitutive model for beam elements with cyclic degradation and damage assessment for advanced dynamic analyses of geotechnical problems. Part II: validation and application to dynamic soil-structure interaction problem. Bulletin of Earthquake Engineering 2017;15(7):2803-2825, 2017.